

Reaction-Induced Spreading of Metal Oxides onto Surfaces of Oxide Supports during Alcohol Oxidation: Phenomenon, Nature, and Mechanisms

Chuan-Bao Wang,[†] Yeping Cai,[‡] and Israel E. Wachs*

Zettlemoyer Center for Surface Studies and Department of Chemical Engineering,
Lehigh University, Bethlehem, Pennsylvania 18015

Received June 18, 1998. In Final Form: December 1, 1998

Reaction-induced spreading of bulk metal oxides onto surfaces of oxide supports during alcohol oxidation, a new phenomenon occurring at temperatures much lower than that required for thermal spreading, has been extensively investigated with Raman spectroscopic and fixed-bed catalytic studies. The reaction-induced spreading kinetics were accelerated by reaction of gaseous components with metal oxides to form mobile complex compounds and found to depend on temperature, gaseous component, metal oxide, and oxide support. Increasing the reaction temperature increases the metal oxide spreading rate. The efficiencies of converting three-dimensional bulk metal oxides into two-dimensional surface metal oxide species by different gaseous components are methanol \gg ethanol $>$ 2-butanol, water \gg oxygen. The high reaction-induced spreading efficiency of methanol is related to the high volatility and stability of its metal–methoxy complexes. Reaction-induced spreading of CrO_3 , MoO_3 , V_2O_5 , Re_2O_7 , and Cr_2O_3 during alcohol oxidation readily occurs on TiO_2 and SnO_2 supports but does not take place on SiO_2 because of the low interaction energy between SiO_2 and surface metal oxide species. Furthermore, reaction-induced spreading does not appear to be influenced by the oxidation state of the spreading metal oxides. The mechanism of reaction-induced spreading proceeds via the reaction of an alcohol with metal cations to form surface mobile and volatile metal–alkoxy complexes and their subsequent transport through surface diffusion and volatilization/readsorption. The reaction-induced spreading of metal oxides is directly reflected in the catalytic properties of such mixed metal oxide materials since the surface metal oxide species are significantly more active than bulk metal oxides for alcohol oxidation reactions. These new findings have important fundamental implications for synergetic effects of metal oxide catalysts composed of physical mixtures and for commercial applications.

Introduction

Surface metal oxide species on oxide supports play a crucial role in the catalytic processes of supported metal oxide catalysts, which have been widely used as catalysts in numerous industrial applications: $\text{MoO}_3/\gamma\text{-Al}_2\text{O}_3$ and $\text{WO}_3/\gamma\text{-Al}_2\text{O}_3$ catalysts for hydrodesulfurization (HDS) and hydro-denitrogenation (HDN),^{1,2} $\text{V}_2\text{O}_5/\text{TiO}_2$ catalysts for *o*-xylene oxidation to phthalic anhydride^{3,4} and selective catalytic reduction (SCR) of NO_x .⁵ The industrial development of supported metal oxide catalysts over the past five decades has been summarized.⁶

Fundamental molecular structural information about the surface metal oxide species has been obtained by a battery of physical and chemical techniques, including Raman spectroscopy, infrared spectroscopy (IR), X-ray photoelectron spectroscopy (XPS), UV diffuse reflectance spectroscopy (UV–vis), solid-state nuclear magnetic resonance (NMR), extended X-ray absorption fine structure (EXAFS), Mössbauer spectroscopy, surface acidity, adsorption, and probe reactions.^{7–10} The reactivity of the



Figure 1. A schematic of thermal spreading of a metal oxide on an oxide support surface.

surface metal oxide species in various supported metal oxide catalysts has been probed by different chemical reactions including methanol oxidation, alkane oxidation, SO_2 oxidation, and the selective catalytic reduction of NO_x .⁶ Correlation of the catalytic reactivity with the corresponding molecular structural information about the surface metal oxide species has elucidated many fundamental issues about the catalytic properties of the surface metal oxide species during catalytic reactions: the roles of terminal $\text{M}=\text{O}$ bonds, bridging $\text{M}-\text{O}-\text{M}'$ bonds, adjacent or neighboring sites, secondary metal oxide additives, support ligands, and preparation methods. The fundamental information obtained from these molecular structure–reactivity relationships has great potential for the molecular design of supported metal oxide catalysts for various catalytic applications.

The formation of two-dimensional metal oxide species on surfaces of oxide supports through thermal spreading of three-dimensional bulk metal oxides, schematically represented in Figure 1, is well documented in the catalysis literature.^{7,8} Thermal spreading is a spontaneous process from a thermodynamics perspective. The driving force for thermal spreading and formation of the surface metal

[†] Current address: Industrial Scientific Corp., 1001 Oakdale Rd., Oakdale, PA 15071-1500.

[‡] Current address: United Catalysts, Inc., 1227 South 12th St., Louisville, KY 40210.

(1) Gates, B. C.; Katzer, J. R.; Schuit, G. C. A. *Chemistry of Catalytic Processes*; McGraw-Hill: New York, 1979.

(2) Topsøe, H. *Surface Properties and Catalysis by Non-Metals*; Bonnelle, J. P., Delmon, B., Derouane E., Eds.; Reidel: Dordrecht and Boston, 1983; p 329.

(3) Bond, G. C.; Vedrine, J. C. *Catal. Today* **1994**, *20*, 1.

(4) Centi, G. *Appl. Catal. A* **1996**, *147*, 267.

(5) Bosch, H.; Janssen, F. *Catal. Today* **1988**, *2*, 369.

(6) Wachs, I. E. *Catalysis* **1997**, *13*, 37.

(7) Haber, J. *Pure Appl. Chem.* **1984**, *56*, 1663.

(8) Xie, Y. C.; Tang, Y. Q. *Adv. Catal.* **1990**, *31*, 1.

(9) Knozinger, H.; Taglauer, E. *Catalysis* **1993**, *10*, 1.

(10) Wachs, I. E. *Catal. Today* **1996**, *27*, 457.

oxide monolayer is a concentration gradient of the dispersed metal oxide or a decrease in the overall system surface free energy. However, its kinetics are constrained because high temperatures are required for surface diffusion or migration of one metal oxide component over the surface of a secondary oxide support to occur at an appreciable rate. In the context of thermal spreading, Tammann temperature ($T_{\text{Tam}} \approx 0.5 T_{\text{mp}}$; T_{mp} = melting point of the bulk metal oxide) is often used to estimate the temperature for thermal treatments.

In contrast, not much information is available on the spreading of metal oxides over oxide supports during catalytic reactions. Gasior et al.¹¹ previously reported the spreading of V_2O_5 over the surface of TiO_2 (anatase) grains in their physical mixture occurring at 360 °C during *o*-xylene oxidation, which was manifested by an increase in both conversion and phthalic anhydride selectivity with reaction time. Cavalli et al.¹² observed that bulk V_2O_5 could spread over the TiO_2 (rutile) surface during amoxidation of toluene to benzonitrile at 320–390 °C. The present paper presents direct evidence that reaction-induced spreading of bulk metal oxides onto oxide supports during alcohol oxidation reactions can occur at temperatures significantly below those required for spontaneous thermal spreading of metal oxides.

2. Experimental Section

2.1. Materials. The TiO_2 (P-25, $\sim 55 \text{ m}^2/\text{g}$), TiO_2 (anatase), and TiO_2 (rutile) supports were purchased from Degussa. The SnO_2 support ($3.7 \text{ m}^2/\text{g}$) was obtained from Aldrich. A fumed Cab-O-Sil SiO_2 support (Cabot, EH-5) with a BET surface area of $380 \text{ m}^2/\text{g}$ was used. For the TiO_2 and SiO_2 supports, treatments with distilled water and subsequent calcination at 550 °C were employed to improve their handling characteristics. MoO_3 , V_2O_5 , CrO_3 , Cr_2O_3 , Re_2O_7 , WO_3 , and Nb_2O_5 were purchased from Aldrich. Methanol (Alfa, Semiconductor Grade), ethanol (McCormick, Absolute-200 Proof), and 2-butanol (Aldrich, 99%) were used as reactants for alcohol oxidation. He (Linde, 99.999%) and O_2 (Linde, 99.99%) were procured from Linde.

2.2. Preparation of Binary Metal Oxide Physical Mixtures. Two methods were used to prepare the physical mixtures: (a) combining an appropriate amount of a metal oxide with an oxide support and pentane (Aldrich, 99+) in a beaker, vibrating for 15 min in an ultrasonic bath, and drying in air for 16 h at 100 °C; (b) mixing a metal oxide and an oxide support by grinding in an agate mortar for 30 min. No further thermal treatments were performed to these physical mixtures.

2.3. Alcohol Oxidation. Alcohol oxidation over the loose powder physical mixture catalysts was performed in a fixed-bed reactor at atmospheric pressure and in the temperature range of 25–400 °C. The details of the reactor system have been previously described.¹³ A reactant stream of CH_3OH (or $\text{C}_2\text{H}_5\text{OH}$)/ $\text{O}_2/\text{He} = 6/13/81$ with a total flow rate of 100 mL/min was used for methanol and ethanol oxidation reactions. For 2-butanol oxidation, a gaseous mixture of 2-butanol/ O_2/He (2.5/13/81, mL/min) was introduced into the reactor. An on-line HP 5890II GC, equipped with a Carboxene-1000 packed and a CP-sil 5 CB capillary columns for TCD and FID detectors, respectively, was used to analyze the reactants and products. At the end of alcohol oxidation reactions, the used catalysts were reoxidized in O_2/He stream at the reaction temperatures for 30 min. For comparison, nonreaction treatments of the physical mixtures were also conducted using different gaseous streams including O_2/He (13/81), $\text{H}_2\text{O}/\text{O}_2/\text{He}$ (3/13/81), and MeOH/He (6/81) with a total flow rate of 100 mL/min at 230 °C.

2.4. Ambient and in Situ Raman Studies. Raman spectra of the physical mixture catalysts after alcohol oxidation or other treatments were recorded using a Spex triplemate spectrometer

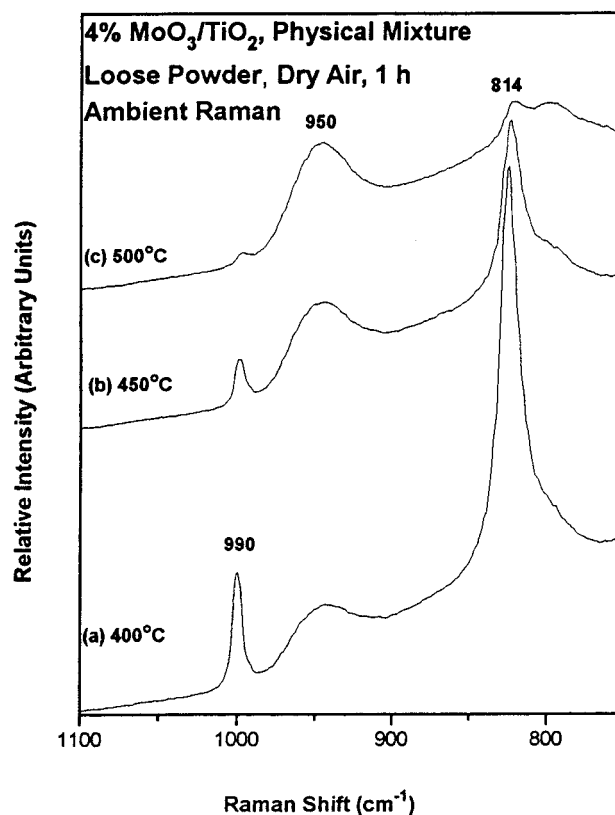


Figure 2. Ambient Raman spectra of a 4% $\text{MoO}_3/\text{TiO}_2$ physical mixture in powder form after 1 h of thermal treatment in dry air at temperatures (a) 400, (b) 450, and (c) 500 °C.

(model 1877), equipped with a Princeton Applied Research OMA III (model 1421) optical multichannel photodiode array detector. The 514.5 nm line of a Spectra Physics model 164 Ar^+ ion laser was used for excitation with a laser power of 25 mW. Raman measurement under dehydrated conditions was achieved by holding the samples stationary.

In situ Raman spectra of the physical mixtures under methanol oxidation reaction conditions were obtained using a Spex triplemate spectrometer (Model 1877) equipped with an Ar^+ laser (Spectra Physics, Model 165), a Princeton Applied Research OMA III (model 1420) optical multichannel photodiode array detector, and an in situ cell.¹⁴ A 100–200 mg self-supporting wafer was placed in the sample holder, which is mounted onto a ceramic shaft rotating at ~ 1500 rpm. Prior to the Raman measurement of a reference spectrum, the wafer was initially heated in an O_2/He (16/84, mL/min) stream at 230 °C for 30 min. A reactant mixture of $\text{CH}_3\text{OH}/\text{O}_2/\text{He}$ (4/16/80, mL/min) was subsequently introduced into the in situ cell at a flow rate of 100 mL/min, and the time dependence of the in situ Raman spectra were obtained. At the end of the methanol oxidation reactions, methanol was removed from the gas stream, which allowed the catalyst to be reoxidized in the O_2/He stream.

3. Results

3.1. Thermal Spreading. MoO_3 on TiO_2 . The ambient Raman spectra of a 4% $\text{MoO}_3/\text{TiO}_2$ physical mixture, in its loose powder form after a 1-h thermal treatment at temperatures of 400–500 °C in dry air, are shown in Figure 2 in the 700–1100 cm^{-1} range. After the 400 °C thermal treatment, the Raman spectrum exhibits sharp 990 and 814 cm^{-1} bands due to crystalline MoO_3 and a broad band at $\sim 950 \text{ cm}^{-1}$, which was previously assigned to the vibration of a hydrated surface molybdenum oxide species.^{15–17} The $\sim 950 \text{ cm}^{-1}$ Raman band intensity of the

(11) Gasior, M.; Haber, J.; Machej, T. *Appl. Catal.* **1987**, *33*, 1.

(12) Cavalli, P.; Cavani, F.; Manenti, I.; Trifiro, F. *Ind. Eng. Chem. Res.* **1987**, *26*, 639.

(13) Deo, G.; Wachs, I. E. *J. Catal.* **1994**, *146*, 335.

(14) Vuurman, M. A.; Hirt, A. M.; Wachs, I. E. *J. Phys. Chem.* **1991**, *95*, 9928.

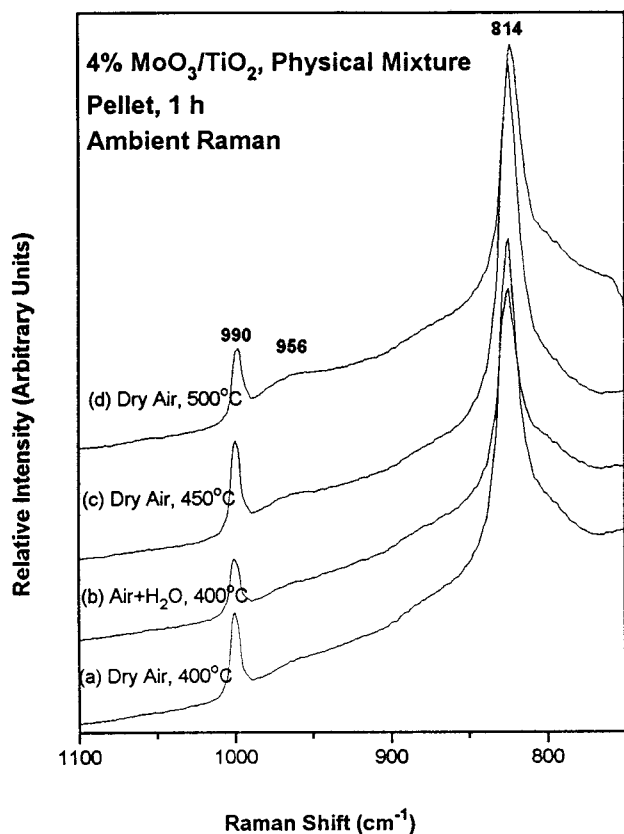


Figure 3. Ambient Raman spectra of a 4% MoO₃/TiO₂ physical mixture in pellet form after 1 h of thermal treatment at the following conditions: (a) 400 °C and dry air; (b) 400 °C and air + H₂O; (c) 450 °C and dry air; (d) 500 °C and dry air.

surface molybdenum oxide species increases with treatment temperatures at the expense of the 990 and 814 cm⁻¹ bands of crystalline MoO₃. After the 1-h thermal treatment at 500 °C, the 990 and 814 cm⁻¹ Raman bands of crystalline MoO₃ almost disappear, and the broad band at 950 cm⁻¹ becomes dominant, indicating that almost complete transformation of bulk MoO₃ into two-dimensional surface molybdenum oxide species occurred. The results are consistent with the previous observation that bulk MoO₃ readily spreads onto the surface of a TiO₂ (P25) support forming a two-dimensional surface metal oxide overlayer when their physical mixtures are thermally treated in dry air at elevated temperatures (400–500 °C).^{7,15–19} The high stability of the surface metal oxide overlayer is the consequence of the strong chemical bonding of the surface molybdena species to the TiO₂ surface.

Similar thermal treatments were applied to the self-supporting wafers of the 4 wt % MoO₃/TiO₂ physical mixture. Interestingly, only a very small amount of the surface molybdenum oxide species formed after the physical mixture pellets were heated at temperatures of 400–500 °C in both dry and wet air, as shown in Figure

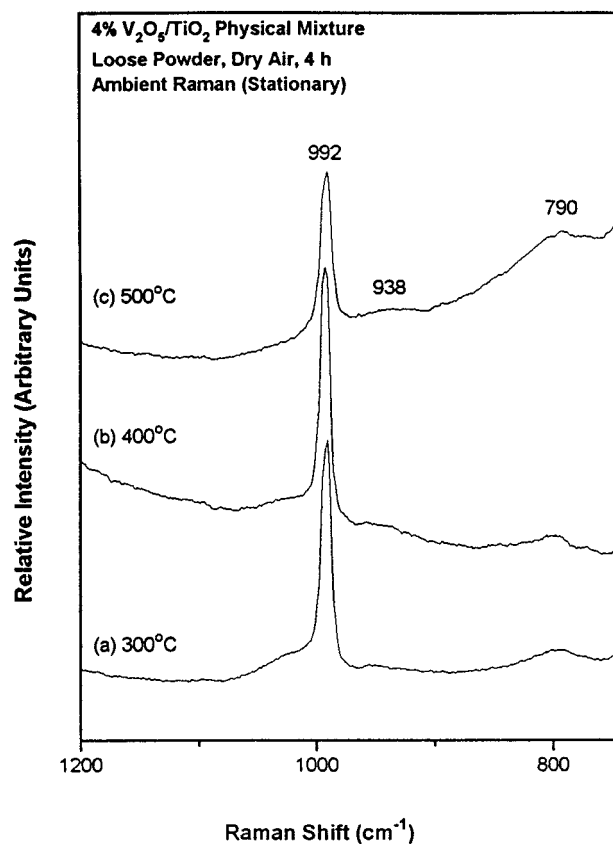


Figure 4. Raman spectra (obtained by holding the samples stationary) of a 4% V₂O₅/TiO₂ physical mixture in powder form after 4 h of thermal treatment in dry air at temperatures (a) 300, (b) 400, and (c) 500 °C.

3. This result suggests that strong mass transfer limitations exist when the physical mixture is in the form of a self-supporting wafer.

V₂O₅ on TiO₂. The Raman spectra of a 4 wt % V₂O₅/TiO₂ physical mixture in both loose powder and pellet forms, after 4-h 300–500 °C treatments in dry air, are presented in Figures 4 and 5, respectively. Dehydration of the surface vanadium oxide species was achieved by holding the samples stationary so that the surface vanadium oxide species can be discriminated from the bulk V₂O₅ crystallites in the Raman spectra. The sharp 990–992 cm⁻¹ Raman band is characteristic of crystalline V₂O₅ and the weak ~790 cm⁻¹ band is due to the first overtone of the 395 cm⁻¹ band of the TiO₂ (anatase) support. The presence of the weak broad features at ~1022 and/or 938 cm⁻¹ due to the surface vanadium oxide species reveals that a small amount of crystalline V₂O₅ had thermally spread onto the TiO₂ support surface when their physical mixture powder samples were treated in dry air at 300–500 °C for 4 h. The ~1022 cm⁻¹ Raman band has been assigned to the V=O vibration of a distorted surface VO₄ species present under dehydrated conditions and the ~938 cm⁻¹ Raman band has been associated with a two-dimensional polymerized VO₄ species.¹⁹

The thermal spreading of V₂O₅ on TiO₂ reported in the literature is somewhat conflicting regarding the treatment conditions under which the surface vanadium oxide species forms.^{16,17,20–22} The discrepancies are probably related to the preparation methods of the physical mixtures, their surface areas, and the presence of surface impurities.²³

3.2. Reaction-Induced Spreading. 3.2.1. MoO₃ on TiO₂, SnO₂, and SiO₂. MoO₃ on TiO₂. The ambient Raman spectra of the 4 wt % MoO₃/TiO₂ physical mixture

(15) Margraf, R.; Leyrer, J.; Taglauer, E.; Knozinger, H. *React. Kinet. Catal. Lett.* **1987**, *35*, 261.

(16) Leyrer, J.; Margraf, R.; Taglauer, E.; Knozinger, H. *Surf. Sci.* **1988**, *201*, 603.

(17) Machej, T.; Haber, J.; Turek, A. M.; Wachs, I. E. *Appl. Catal.* **1991**, *70*, 115.

(18) Haber, J.; Machej, T.; Grabowski, R. *Solid State Ionics* **1989**, *32/33*, 887.

(19) Xie, Y.; Gui, L.; Liu, Y.; Zhao, B.; Yang, N.; Zhang, Y.; Guo, Q.; Duan, L.; Huang, H.; Cai, X.; Tang, Y. *Proc. 8th Int. Cong. Catal.*; Dechema, Frankfurt, and Verlag Chemie: Weinheim, 1984; Vol. V, p 147.

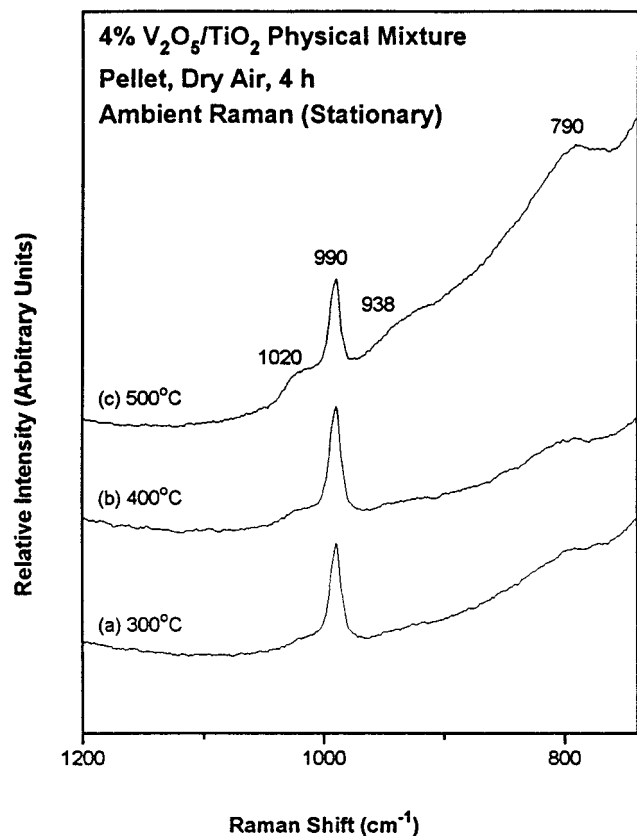


Figure 5. Raman spectra (obtained by holding the samples stationary) of a 4% V_2O_5/TiO_2 physical mixture in pellet form after 4 h of thermal treatment in dry air at conditions (a) 300, (b) 400, and (c) 500 °C.

samples after 4 h of methanol oxidation at 25 to 230 °C are shown in Figure 6. After methanol oxidation at 25 °C, the Raman spectrum was essentially identical to that of crystalline MoO_3 (Figure 6a). Methanol oxidation even at 100 °C, however, leads to the formation of a considerable amount of surface molybdenum oxide species on TiO_2 , evidenced by the presence of the broad Raman band at $\sim 950\text{ cm}^{-1}$ shown in Figure 6b. It must be noted that the sensitivity for detection of crystalline MoO_3 is 17 times more than that for detection of surface molybdenum oxide species.^{24a} Increasing the reaction temperature from 100 to 230 °C leads to the dominance of the surface molybdenum oxide species only with a trace of crystalline MoO_3 present in the final catalyst mixture (see Figure 6d). The spreading of bulk MoO_3 onto the TiO_2 support during methanol oxidation occurred at temperatures that are much lower than the Tammann temperature (261 °C) of crystalline MoO_3 .

Direct evidence for reaction-induced spreading also comes from the in situ Raman studies during methanol oxidation, as shown in Figure 7 over a catalyst pellet consisting of a 4% MoO_3/TiO_2 physical mixture at 230 °C. Prior to methanol oxidation, the Raman spectrum only possesses the strong Raman bands of crystalline MoO_3 at 814 and $\sim 988\text{ cm}^{-1}$ (see Figure 7a). Upon exposure to the

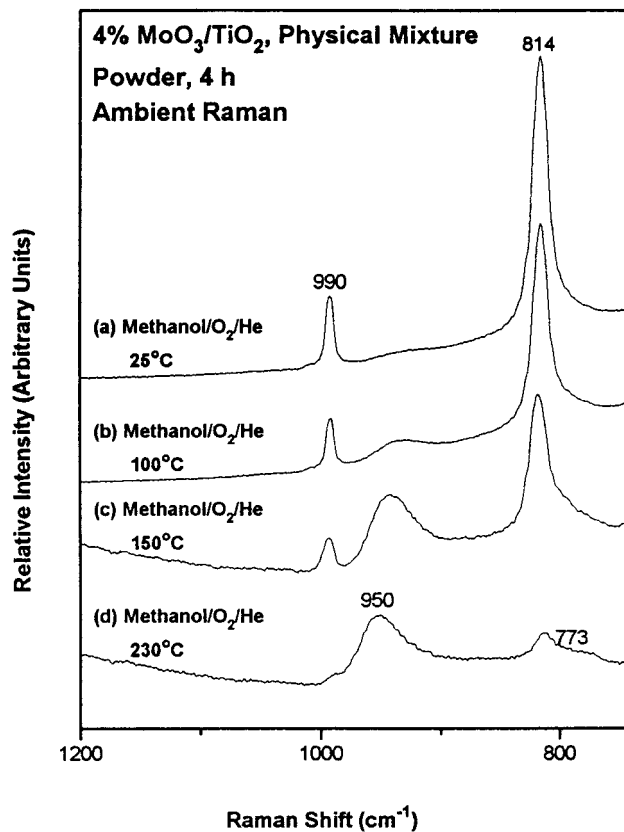


Figure 6. Ambient Raman spectra of a 4% MoO_3/TiO_2 physical mixture in powder form after 4 h of methanol oxidation at reaction temperatures (a) 25, (b) 100, (c) 150, and (d) 230 °C.

methanol oxidation reaction conditions, the sharp Raman bands due to crystalline MoO_3 slowly diminish with reaction time and a new broad Raman band at 969 cm^{-1} is formed (see Figure 7b–e). The in situ Raman band at 969 cm^{-1} has previously been assigned to a surface molybdenum oxide coordinated to a methoxy species.^{24b} When the mixture was switched to an O_2/He stream, the Raman band at 969 cm^{-1} shifted toward 990 cm^{-1} due to the decomposition of the surface molybdate methoxy complex to a dehydrated surface molybdenum oxide species (see spectra f and g of Figure 7). Simultaneously, there was also an increase in the crystalline MoO_3 814 and $\sim 988\text{ cm}^{-1}$ Raman bands due to the oxidation of the partially reduced bulk MoO_3 particles during the methanol oxidation reaction. Further increase of the reaction temperature to 300 °C for about an hour resulted in the complete disappearance of the crystalline MoO_3 Raman bands and only the appearance of the Raman band associated with the surface molybdenum oxide species (not shown here). Further oxidation of the sample at 300 °C again resulted in the appearance of weak crystalline MoO_3 Raman bands revealing that some residual reduced MoO_3 crystallites still remained and that higher temperature treatment or longer reaction time is required for the complete spreading of bulk MoO_3 on the titania support.

The reaction-induced spreading of MoO_3 on TiO_2 is also reflected by the variation of the methanol oxidation catalytic properties of the physical mixture catalysts with reaction time during methanol oxidation. The dependence of the methanol oxidation activity and formaldehyde selectivity on reaction time was studied over 60 mg of a 4% MoO_3/TiO_2 physical mixture catalyst at 230 °C and is presented in Figure 8A. The methanol oxidation activity has been normalized to the number of methanol molecules

(20) Haber, J. *Surface Properties and Catalysis by Non-Metals*; Bonnelle, J. P., Delmon, B., Derouane E., Eds.; Reidel: Dordrecht and Boston, 1983; p 1.

(21) Haber, J.; Machej, T.; Czeppe, T. *Surf. Sci.* **1985**, *151*, 301.

(22) Honicke, D.; Xu, J. *J. Phys. Chem.* **1988**, *92*, 4699.

(23) Hausinger, G.; Schmelz, H.; Knozinger, H. *Appl. Catal.* **1988**, *39*, 267.

(24) (a) Baltrus, J. P.; Makovsky, L. E.; Stencel, J. M.; Hercules, D. M. *Anal. Chem.* **1985**, *57*, 2500. (b) Hu, H.; Wachs, I. E. *J. Phys. Chem.* **1995**, *99*, 10911.

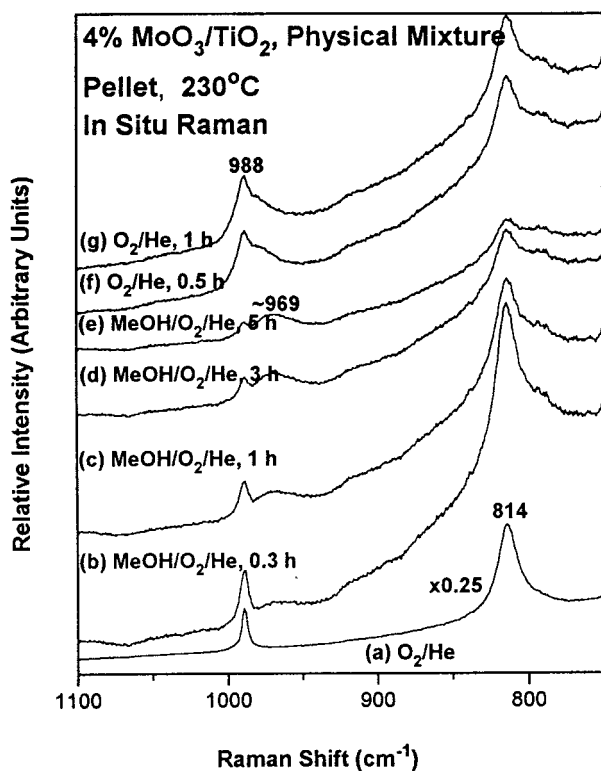


Figure 7. In situ Raman spectra of a 4% MoO₃/TiO₂ physical mixture in pellet form during methanol oxidation at 230 °C: (a) flowing O₂/He; (b) methanol oxidation, 20 min; (c) methanol oxidation, 1 h; (d) methanol oxidation, 3 h; (e) methanol oxidation, 5 h; (f) flowing O₂/He, 0.5 h; (g) flowing O₂/He, 1 h.

converted per total molybdenum atoms per second (i.e., the turnover frequency (TOF)). The catalytic activity of the physical mixture increases with reaction time from an initial TOF of 0.02 s⁻¹ at 5 min to a final TOF of 0.041 s⁻¹ at 455 min and asymptotically approaches the catalytic activity (TOF = 0.045 s⁻¹) of a 4% MoO₃/TiO₂ catalyst prepared by alkoxide impregnation (100% dispersed Mo). The selectivity to formaldehyde also increases over the initial 70 min and approaches the formaldehyde selectivity (73%) of the 4% MoO₃/TiO₂ catalyst prepared by alkoxide impregnation. Previous investigations have revealed that the surface molybdenum oxide species is the active site for methanol oxidation to formaldehyde and that it possesses a much higher TOF than bulk MoO₃.^{24b} The simultaneous increase in both catalytic activity and formaldehyde selectivity of the 4% MoO₃/TiO₂ physical mixture catalyst with reaction time directly corresponds to the gradual spreading of bulk MoO₃ onto the TiO₂ support surface. The corresponding Raman spectrum of the 4% MoO₃/TiO₂ physical mixture catalyst after methanol oxidation (shown in Figure 8B) confirms that almost complete transformation of crystalline MoO₃ into surface molybdenum oxide species has occurred.

The studies were further extended to examine the effects of higher alcohol oxidation (ethanol and 2-butanol) on reaction-induced spreading of MoO₃ on TiO₂. The Raman band intensity ratios (I_{950}/I_{990}) of the surface molybdenum oxide species to crystalline MoO₃ in the 4% MoO₃/TiO₂ physical mixture samples after alcohol (methanol, ethanol, and 2-butanol) oxidation reactions, at 230 °C for 4 h, are represented in Figure 9. For comparison, the Raman band intensity ratios (I_{950}/I_{990}) after treatments with O₂/He, H₂O/O₂/He and methanol/He gas streams at 230 °C for 4 h are also presented in Figure 9. The higher the I_{950}/I_{990} ratios are, the more crystalline MoO₃ has spread onto the TiO₂

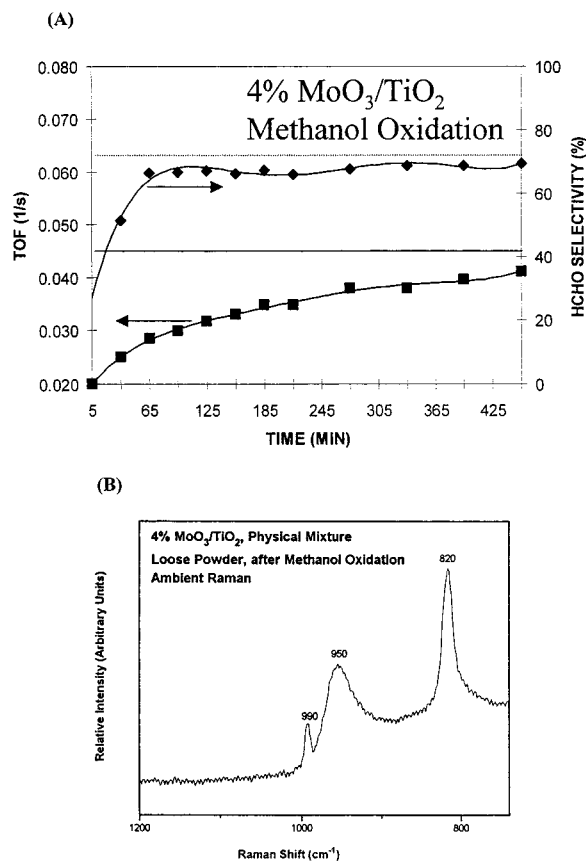


Figure 8. (A) Plot of methanol oxidation TOF and formaldehyde selectivity versus reaction time over a 4% MoO₃/TiO₂ physical mixture catalyst in powder form in comparison with the methanol oxidation TOF (represented by solid line) and formaldehyde selectivity (represented by dot line) of a 4% MoO₃/TiO₂ supported catalyst prepared by impregnation (100% dispersed Mo); (B) Ambient Raman spectrum of the 4% MoO₃/TiO₂ physical mixture catalyst after methanol oxidation.

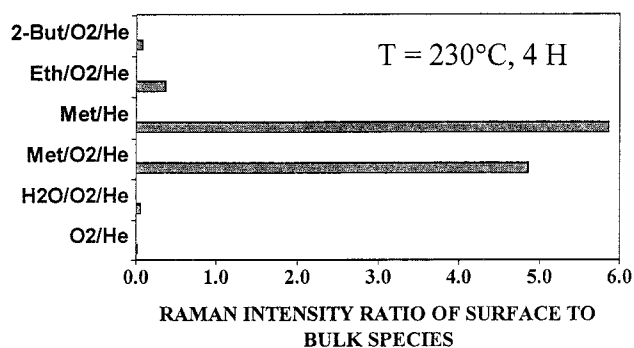


Figure 9. Dependence of Raman band intensity ratios (I_{950}/I_{990}) of surface molybdate to crystalline MoO₃ in a 4 wt % MoO₃/TiO₂ physical mixture on alcohol oxidation and other gaseous stream treatment conditions at 230 °C for 4 h.

surface as a two-dimensional surface MoO_x species. These results demonstrate that the induced spreading of MoO₃ on TiO₂ follows the trend methanol ≫ ethanol > 2-butanol, water. Furthermore, an oxygen-free methanol environment is also highly favorable for the transformation of crystalline MoO₃ into the surface molybdenum oxide species, suggesting that methanol is the key component that is associated with the bulk MoO₃ spreading onto the TiO₂ support surface during methanol oxidation.

The reaction-induced spreading of bulk MoO₃ onto TiO₂ is also reflected in the continuous increase in the higher alcohol (ethanol and 2-butanol) conversion with reaction

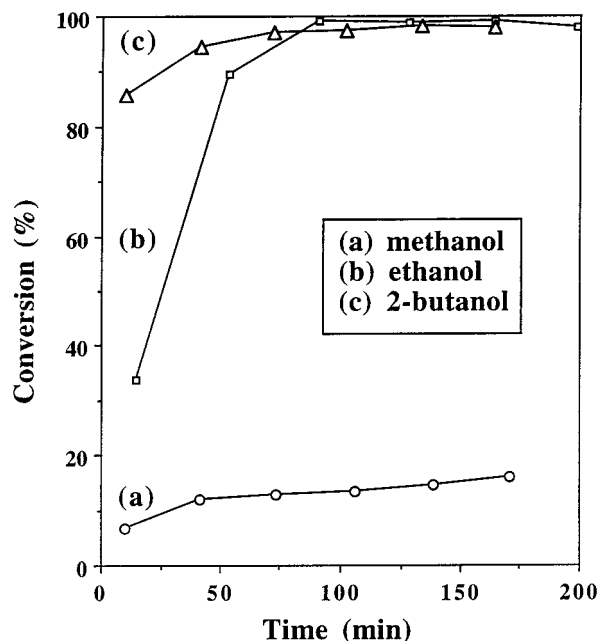


Figure 10. Alcohol conversions over a 4% $\text{MoO}_3/\text{TiO}_2$ physical mixture in powder form at 230 °C as a function of reaction time: (a) methanol oxidation; (b) ethanol oxidation; (c) 2-butanol oxidation.

time, as shown in Figure 10. For comparison, the conversion data for methanol oxidation is also plotted in Figure 10. The methanol conversion over the 4% $\text{MoO}_3/\text{TiO}_2$ physical mixture continuously increased from about 8 to 16% during the first 3 h of reaction. The ethanol and 2-butanol conversions also increased continuously with reaction time but the higher alcohols were more active than methanol due to their weaker $\alpha\text{-C-H}$ bonds. Thus, the increase in alcohol conversion as a function of reaction time over the $\text{MoO}_3/\text{TiO}_2$ physical mixture catalysts is directly related to the transformation of crystalline MoO_3 into the surface molybdenum oxide species on the TiO_2 support.

MoO_3 on SnO_2 . The reaction-induced spreading of bulk MoO_3 also readily occurs on different oxide supports during methanol oxidation at mild temperatures. The in situ Raman spectra of a 1 wt % $\text{MoO}_3/\text{SnO}_2$ physical mixture acquired during methanol oxidation and treatments in an O_2/He stream at 230 °C are shown in Figure 11. The Raman features at 630 and 775 cm^{-1} are due to the SnO_2 support.²⁵ The sharp 990, 814, and 667 cm^{-1} Raman bands, characteristic of crystalline MoO_3 , nearly disappeared after a half hour of methanol oxidation at 230 °C, and a broad band at ~ 970 cm^{-1} due to a surface molybdenum oxide methoxy species^{24b} is observed (see Figure 11c). Subsequent reoxidation with O_2/He at 230 °C slightly increases the band intensities of both the surface molybdenum oxide species and crystalline MoO_3 (see Figure 11d).

MoO_3 on SiO_2 . In the case of $\text{MoO}_3/\text{SiO}_2$ physical mixtures, it is expected that no spreading should be observed during methanol oxidation since the surface molybdenum oxide species are not stable under methanol oxidation reaction conditions.²⁶ The methanol oxidation TOFs of a 4 wt % $\text{MoO}_3/\text{SiO}_2$ physical mixture catalyst as a function of reaction time at 230 °C are shown in Figure

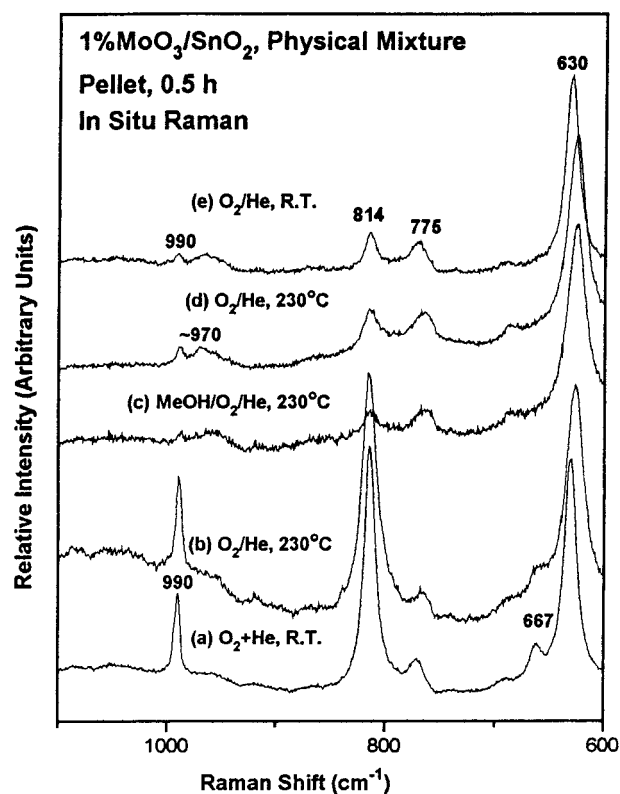


Figure 11. In situ Raman spectra of a 1% $\text{MoO}_3/\text{SnO}_2$ physical mixture in pellet form during methanol oxidation: (a) flowing O_2/He , room temperature; (b) flowing O_2/He , 230 °C, 30 min; (c) methanol oxidation, 230 °C, 30 min; (d) flowing O_2/He , 230 °C, 30 min; (e) flowing O_2/He , room temperature.

12A. In contrast to the results for the 4 wt % $\text{MoO}_3/\text{TiO}_2$ physical mixture, the methanol oxidation activity of the 4 wt % $\text{MoO}_3/\text{SiO}_2$ physical mixture does not increase with reaction time and does not asymptotically approach the TOF (0.07 s^{-1}) of a 4 wt % $\text{MoO}_3/\text{SiO}_2$ catalyst prepared by alkoxide impregnation (100% dispersed Mo). The formaldehyde selectivity data were not obtained due to the low methanol conversion. Thus, the catalytic results suggest that crystalline MoO_3 does not spread onto the SiO_2 support during methanol oxidation. The corresponding Raman spectra of the 4 wt % $\text{MoO}_3/\text{SiO}_2$ physical mixture catalyst before and after methanol oxidation (presented in Figure 12B) show that only the Raman bands due to crystalline MoO_3 are observed and that the Raman bands due to surface molybdenum oxide species are not present. The Raman bands of crystalline MoO_3 after methanol oxidation are much weaker than those before methanol oxidation, suggesting that a significant amount of crystalline MoO_3 was lost from the 4 wt % $\text{MoO}_3/\text{SiO}_2$ physical mixture catalyst. This is further confirmed by the observation that a large amount of crystalline MoO_3 was found deposited at the cooler exit of the reactor and that the color of the 4 wt % $\text{MoO}_3/\text{SiO}_2$ physical mixture catalyst after methanol oxidation was closer to that of pure SiO_2 .

3.2.2. V_2O_5 on TiO_2 , SnO_2 , and SiO_2 . V_2O_5 on TiO_2 . The in situ Raman spectra of a self-supported wafer consisting of a 4% $\text{V}_2\text{O}_5/\text{TiO}_2$ physical mixture during methanol oxidation at 230 °C are shown in Figure 13. The starting sample only exhibits the Raman bands of crystalline V_2O_5 at about 990 cm^{-1} and the titania support at about 790 cm^{-1} (see Figure 13a). Exposure of the 4% $\text{V}_2\text{O}_5/\text{TiO}_2$ catalyst to the methanol oxidation reaction at 230 °C completely removes the Raman bands of the V_2O_5

(25) Stampfl, S. R.; Chen, C.; Dumesic, J. A.; Niu, C.; Hill, C. G., Jr. *J. Catal.* **1987**, *105*, 445.

(26) Jehng, J. M.; Hu, H.; Gao, X.; Wachs, I. E. *Catal. Today* **1996**, *28*, 335.

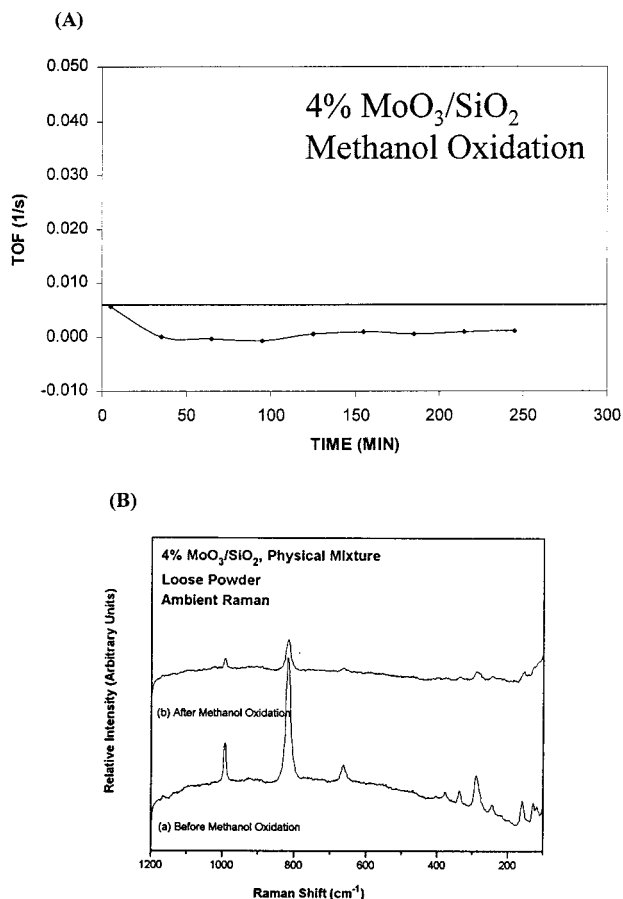


Figure 12. (A) Plot of methanol oxidation TOF versus reaction time over a 4% MoO₃/SiO₂ physical mixture catalyst in powder form in comparison with the TOF of a 4% MoO₃/SiO₂ supported catalyst prepared by impregnation (100% dispersed Mo). (B) Ambient Raman spectra of the 4% MoO₃/SiO₂ physical mixture catalyst (a) before and (b) after methanol oxidation.

crystals and no new bands due to surface vanadia species are observed (see Figure 13b–d). The complete absence of any vanadia Raman bands suggests that the vanadia component of the catalyst was reduced since reduced vanadia gives rise to very weak Raman bands.²⁷ Reoxidation of the 4% V₂O₅/TiO₂ physical mixture catalyst wafer resulted in the appearance of a new Raman band at 1022 cm⁻¹ associated with surface vanadia species (see Figure 13e,f)^{14,17,28} and the complete absence of crystalline V₂O₅ particles. Thus, the in situ Raman studies demonstrate that crystalline V₂O₅ completely transformed into the surface vanadium oxide species during methanol oxidation at a very mild temperature, 230 °C.

The structural changes in the V₂O₅/TiO₂ physical mixture catalyst also result in corresponding changes in the methanol oxidation activity and selectivity patterns of this catalyst. The evolution of the activity and formaldehyde selectivity with reaction time is observed during methanol oxidation in a fixed bed reactor with 10 mg of the 4% V₂O₅/TiO₂ physical mixture at 230 °C, shown in Figure 14A. The catalytic activity of the V₂O₅/TiO₂ physical mixture catalyst continuously increases with reaction time during the initial methanol oxidation period. When the reaction time exceeded 155 min, corresponding to the time required for complete spreading of V₂O₅ on TiO₂ to occur,

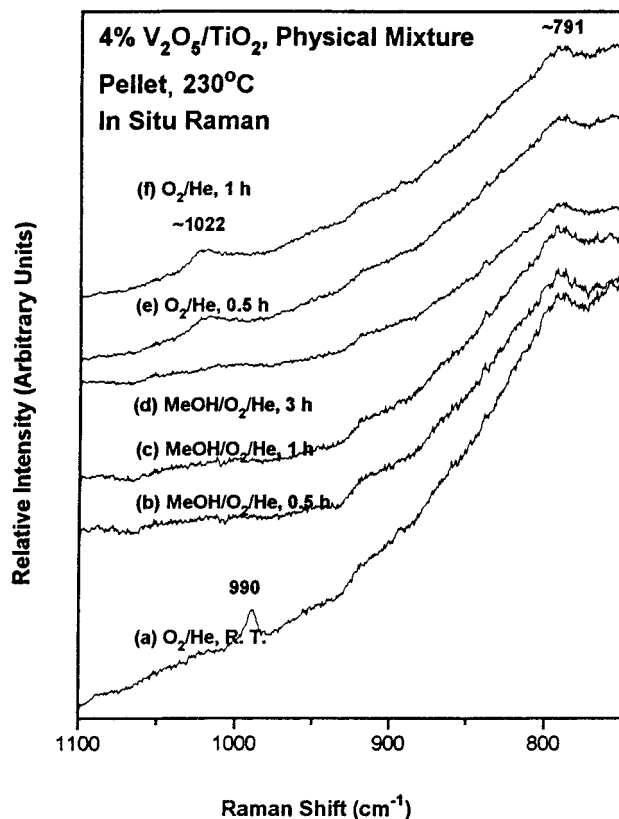


Figure 13. In situ Raman spectra of a 4% V₂O₅/TiO₂ physical mixture in pellet form during methanol oxidation: (a) flowing O₂/He, room temperature; (b) methanol oxidation, 230 °C, 0.5 h; (c) methanol oxidation, 230 °C, 1 h; (d) methanol oxidation, 230 °C, 3 h; (e) flowing O₂/He, 230 °C, 0.5 h; (f) flowing O₂/He, 230 °C, 1 h.

a constant activity is observed, which is the same as that (TOF = 0.185 s⁻¹) of a 4% V₂O₅/TiO₂ catalyst prepared by alkoxide impregnation (100% dispersion of vanadium). The formaldehyde selectivity remained essentially constant at all the conversion levels. The corresponding Raman spectrum of the 4% V₂O₅/TiO₂ physical mixture after methanol oxidation reveals that complete spreading of crystalline V₂O₅ onto the TiO₂ surface as a two-dimensional vanadium oxide species occurred, as shown in Figure 14B. The surface VO_x species are characterized by the broad Raman bands at 1020 and ~930 cm⁻¹.

The influence of different gaseous environments on the spreading of V₂O₅ on TiO₂ is compared in Figure 15. Exposure of the 4 wt % V₂O₅/TiO₂ physical mixture catalyst to the O₂/He and H₂O/O₂/He steams at 230 °C for 4 h resulted in a broad and ill-defined band at about 938 cm⁻¹, in addition to the sharp strong band at 990 cm⁻¹ due to crystalline V₂O₅ (Figure 15b,c). The Raman band ~938 cm⁻¹ band has been assigned to a hydrated polymerized surface vanadium oxide species based on previous Raman and NMR studies.^{17,29} Upon being exposed to methanol and 2-butanol oxidation conditions at 230 °C for 4 h, the sharp 990 cm⁻¹ band of crystalline V₂O₅ almost completely disappeared and a broad band of considerable intensity at about 1018 and a weak band at 938 cm⁻¹ were observed for the sample after methanol oxidation (Figure 15d) and only the 938 cm⁻¹ band was present in the sample after 2-butanol oxidation (Figure 15e) since the 1018 cm⁻¹ band is masked by the strong fluorescence. The 1018 cm⁻¹ band is due to dehydrated surface vanadium oxide species, as

(27) Wachs, I. E.; Jehng, J. M.; Deo, G.; Weckhuysen, B. M.; Gulianti, V. V.; Benziger, J. B. *Catal. Today* **1996**, *32*, 47.

(28) Went, G.; Oyama, S. T.; Bell, A. T. *J. Phys. Chem.* **1990**, *94*, 4240.

(29) Eckert, H.; Wachs, I. E. *J. Phys. Chem.* **1989**, *93*, 679.

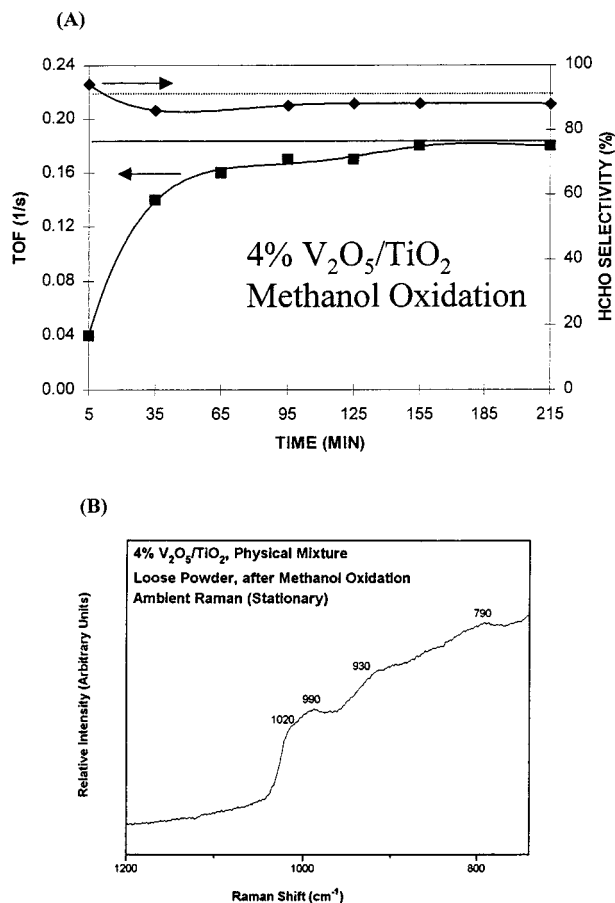


Figure 14. (A) Plot of methanol oxidation TOF and formaldehyde selectivity versus reaction time over a 4% V₂O₅/TiO₂ physical mixture catalyst in powder form in comparison with the TOF (represented by solid line) and formaldehyde selectivity (represented by dot line) of a 4% V₂O₅/TiO₂ supported catalyst prepared by impregnation (100% dispersed V). (B) Raman spectrum (obtained by holding the sample stationary) of the 4% V₂O₅/TiO₂ physical mixture catalyst after methanol oxidation.

a result of laser induced dehydration.¹⁷ Compared to the other samples, the sample exposed to the 2-butanol oxidation conditions possessed strong fluorescence in the 1000 cm⁻¹ region. The above results suggest that the efficiency of the reaction-induced spreading for the V₂O₅/TiO₂ physical mixtures follows the trend: methanol, 2-butanol >> water, oxygen.

The alcohol conversions over the 4% V₂O₅/TiO₂ physical mixture catalyst during alcohol oxidation are plotted against reaction time and shown in Figure 16. The continuous increase of alcohol oxidation (methanol, ethanol, and 2-butanol) activity with time is consistent with the structural transformation of the 4 wt % V₂O₅/TiO₂ physical mixture catalyst. For methanol oxidation, the methanol conversion continuously increased from about 18 to 37% during the first 115 min of reaction and then exhibited a very sharp increase to ~100% at about 140 min. The jump in methanol conversion was accompanied by an increase in the catalyst bed temperature from 230 to 244 °C due to the exothermic heat of reaction.

The reaction-induced spreading of bulk V₂O₅ can occur on both TiO₂ (rutile) and TiO₂ (anatase) supports. The Raman spectra (not shown here) of a 1 wt % V₂O₅/TiO₂ (rutile or anatase) physical mixtures after 4 h of methanol oxidation at 230 °C exhibit a broad Raman band at about 930 cm⁻¹ (see Table 2), characteristic of a polymerized surface vanadium oxide species.^{17,29} The sharp 990 cm⁻¹

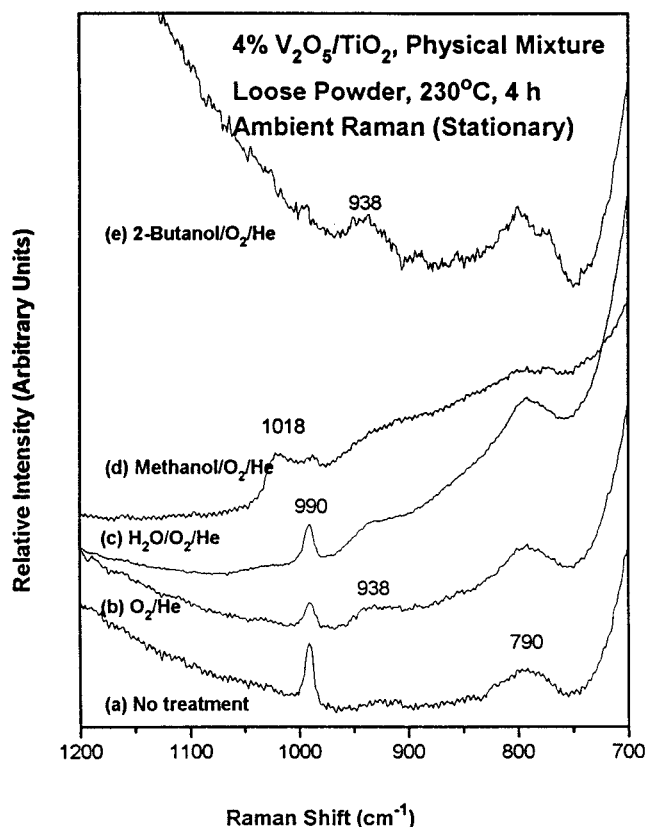


Figure 15. Raman spectra (obtained by holding the samples stationary) of a 4% V₂O₅/TiO₂ physical mixture in powder form after 4 h of alcohol oxidation and other gaseous stream treatment conditions: (a) no treatment; (b) O₂/He, 230 °C; (c) H₂O/O₂/He, 230 °C; (d) methanol oxidation, 230 °C; (e) 2-butanol oxidation, 230 °C.

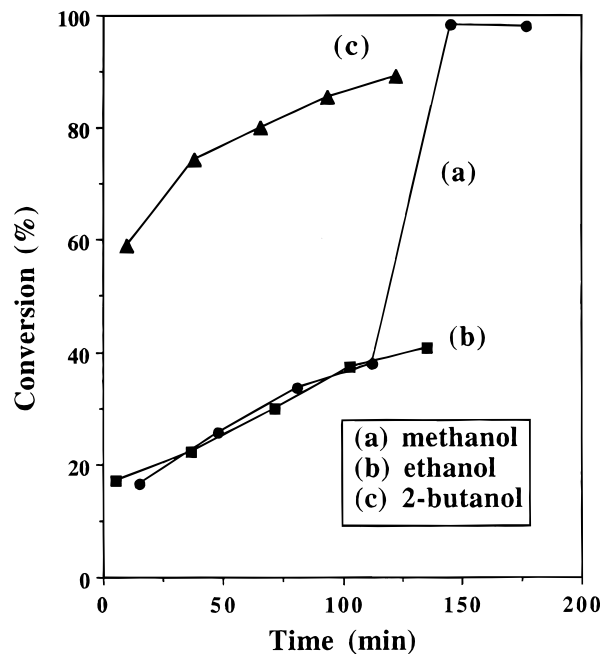


Figure 16. Alcohol conversions over a 4% V₂O₅/TiO₂ physical mixture in powder form at 230 °C as a function of reaction time: (a) methanol oxidation; (b) ethanol oxidation; (c) 2-butanol oxidation.

band of crystalline V₂O₅ is absent for both samples, demonstrating that crystalline V₂O₅ has completely spread onto the surfaces of both rutile and anatase TiO₂ supports as surface vanadia species.

V₂O₅ on SnO₂. The in situ Raman studies were also carried out on a 4 wt % V₂O₅/SnO₂ physical mixture catalyst during methanol oxidation at 230 °C (not shown here). After 1.5 h of methanol oxidation, all the Raman bands related to the vanadia component of the catalyst disappeared, suggesting the vanadia component was reduced in the methanol oxidation environment. Reoxidation with O₂/He at 230 °C for 0.5–1 h reestablished a broad Raman band at 1025 cm⁻¹ due to the dehydrated surface vanadium oxide species (see Table 2). This experiment illustrates that reaction-induced spreading of crystalline V₂O₅ on the SnO₂ support occurred during methanol oxidation at a mild temperature. However, thermal spreading of V₂O₅ on SnO₂ was not observed to occur.²²

V₂O₅ on SiO₂. Similar to the MoO₃/SiO₂ system, the reaction-induced spreading of bulk V₂O₅ on SiO₂ did not occur either. The methanol oxidation TOFs as a function of reaction time for a 4 wt % V₂O₅/SiO₂ physical mixture catalyst at 230 °C are much lower than the TOF of a 4 wt % V₂O₅/SiO₂ catalyst prepared by impregnation (100% dispersed V), suggesting that the surface vanadium oxide species do not form on SiO₂. The selectivity data were not reported because of the low methanol conversion. The corresponding Raman spectra (not shown here) of the 4% V₂O₅/SiO₂ physical mixture before and after methanol oxidation reveal that crystalline V₂O₅ has been completely removed from the physical mixture catalyst during methanol oxidation, also evidenced by the fact that the final catalyst exhibits the same color as pure SiO₂.

3.2.3. CrO₃, Cr₂O₃, Re₂O₇, WO₃, and Nb₂O₅ on TiO₂. Experiments were also performed to examine the reaction-induced spreading of other metal oxides (CrO₃, Cr₂O₃, Re₂O₇, WO₃, and Nb₂O₅) on the TiO₂ (P-25) support. The results for the 4% M_xO_y (M = Cr, Re, W, and Nb)/TiO₂ physical mixtures after 2 h of methanol oxidation at 230 and 400 °C are summarized in Table 2 together with above other systems.

The Raman spectrum of a spinning CrO₃/TiO₂ catalyst pellet exhibits only a band at 790 cm⁻¹ due to the TiO₂ support. When the sample was stationary, dehydration induced by the laser beam resulted in a new band at ~1000 cm⁻¹, corresponding to a dehydrated surface chromium oxide species.^{30,31} Under hydrated conditions, this band would shift to ~880 cm⁻¹, which was masked by the high background in this region of the spectrum.

Similar to the CrO₃/TiO₂ catalyst, the Cr₂O₃/TiO₂ catalyst (stationary) also exhibits a weak band at ~1000 cm⁻¹, corresponding to the dehydrated surface chromium oxide species. Interestingly, this result suggests that crystalline Cr₂O₃ has spread onto the TiO₂ surface during methanol oxidation.

The Raman bands of the Re₂O₇/TiO₂ physical mixture after methanol oxidation occurred at ~980 and ~920 cm⁻¹ when the sample was spun. The 980 cm⁻¹ band shifts to ~990 cm⁻¹ due to partial dehydration induced by the laser beam when the sample was held stationary. This behavior is reversible, as demonstrated by the 990 cm⁻¹ Raman band shifting back to 980 cm⁻¹ when the sample is rotated. The current observation is consistent with the previous findings for the Re₂O₇/Al₂O₃ catalysts,³² suggesting that bulk Re₂O₇ has spread onto the TiO₂ surface during methanol oxidation.

The Raman spectra of the 4% Nb₂O₅/TiO₂ physical mixture after 2 h of methanol oxidation at 230 and 400

°C showed that Raman spectra measured by spinning the samples or holding them stationary are almost identical, possessing only the ~790 cm⁻¹ band due to TiO₂. Absence of a ~980 cm⁻¹ band due to the dehydrated surface niobium oxide species and a ~890 cm⁻¹ band due to the hydrated surface niobium oxide species^{10,33} indicates that Nb₂O₅ did not spread onto the surface TiO₂ during methanol oxidation.

The Raman spectra of the WO₃/TiO₂ physical mixture catalyst exhibits very sharp bands at 800 and 713 cm⁻¹, which are characteristic of crystalline WO₃ particles. The Raman band due to the surface tungsten oxide species (expected at 1010 cm⁻¹ under dehydrated conditions and ~980 cm⁻¹ under hydrated conditions)^{34,35} is not observed, implying that reaction-induced spreading of WO₃ on TiO₂ does not occur for this system under these mild reaction conditions.

4. Discussion

4.1. Thermal Spreading. It is well-known that surface diffusion or migration has played an important role in agglomeration, sintering, and active-component redistribution in heterogeneous catalysts.^{36,37} Thermal spreading is believed to be related to surface migration or diffusion of one component over the surfaces of an oxide support,³⁸ and high temperature is required to overcome the intrinsic resistance coming from the generally high lattice energies of active components. As a rule, thermal treatment temperatures must be higher than the Tammann temperature of the metal oxide in order for surface diffusion to occur at an appreciable rate. When the 4% MoO₃/TiO₂ physical mixture is heated at 400–500 °C, it is not surprising that a significant amount of crystalline MoO₃ has transformed into surface molybdenum oxide species (see Figure 2) because the heating temperatures are much higher than the Tammann temperature of MoO₃ ($T_{\text{Tamm}} = 261$ °C). The higher the heating temperature, the more the crystalline MoO₃ transforms into the surface molybdenum oxide species due to higher surface diffusion or migration rate at higher temperatures. In contrast to prediction, only a small amount of V₂O₅ spread onto TiO₂ after their physical mixture was heated at 300–500 °C for 4 h in dry air (see Figures 4 and 5) even though the heating temperatures were also much higher than the Tammann temperature of crystalline V₂O₅ (206 °C). Conflicting results were reported in the literature regarding thermal dispersion of the V₂O₅/TiO₂ system. Haber et al.³⁹ and Honicke et al.²² did observe significant spreading of V₂O₅ on TiO₂ after thermal treatment in dry air at 450 °C for 1 h or 500 °C for 48 h for their physical mixtures made by grinding in an agate mortar. In contrast, Leyrer et al.¹⁶ showed that thermal spreading of V₂O₅ on TiO₂ did not occur after a hand-grinding physical mixture was thermally treated at 500 °C for 48 h in dry O₂. Hausinger et al.²³ demonstrated that the spreading tendency of V₂O₅ on TiO₂ was influenced by mixing methods of their physical mixtures.

4.2. Reaction-Induced Spreading. 4.2.1. Factors Influencing Reaction-Induced Spreading. Effect of Temperature. The temperature range at which metal

(33) (a) Jehng, J. M.; Wachs, I. E. *Catal. Today* **1993**, *16*, 417. (b) Jehng, J. M.; Wachs, I. E. *J. Phys. Chem.* **1991**, *95*, 7373.

(34) Deo, G.; Wachs, I. E. *J. Phys. Chem.* **1991**, *95*, 5889.

(35) Kim, D. S.; Ostromecki, M.; Wachs, I. E. *J. Mol. Catal. A* **1996**, *106*, 93.

(36) Ruckenstein, E.; Lee, S. H. *J. Catal.* **1987**, *104*, 259.

(37) Wanke, S. E.; Flynn, P. C. *Catal. Rev. Sci. Eng.* **1975**, *12*, 93.

(38) Wang, C. B.; Xie, Y. C.; Tang, Y. Q. *Sci. China* **1994**, *37*, 1458.

(39) Haber, J.; Machej, T.; Serwicka, E. M.; Wachs, I. E. *Catal. Lett.* **1995**, *32*, 101.

(30) Hardcastle, F. D.; Wachs, I. E. *J. Mol. Catal.* **1988**, *46*, 173.

(31) Vuurman, M. A.; Wachs, I. E.; Stufkens, D. J.; Oskam, A. *J. Mol. Catal.* **1993**, *80*, 209.

(32) Hardcastle, F. D.; Wachs, I. E. *J. Mol. Catal.* **1988**, *46*, 15.

Table 1. Surface Free Energies, Melting Points, and Tammann Temperatures of Metal Oxides and Oxide Supports⁹

oxide	$\gamma/10^{-6} \text{ J cm}^{-2}$	$T_{\text{melt}}/^\circ\text{C}$	$T_{\text{Tamm}}/^\circ\text{C}$
CrO ₃		197	-38
Re ₂ O ₇	3-4	297	12
V ₂ O ₅	8-9	690	209
MoO ₃	5-7	795	261
WO ₃	10	1474	600
Nb ₂ O ₅		1512	620
Cr ₂ O ₃		2454	1081
TiO ₂	28-38	1900	813
SnO ₂		1630	679
SiO ₂	39	1713	720
Al ₂ O ₃	68-70	2054	890
MgO	110-115	2800	1263
ZnO	90	1975	851
ZrO ₂	59-80	2715	1221

oxides spread over oxide supports allows for the discrimination between reaction-induced spreading and thermal spreading. Thermal spreading of crystalline MoO₃ onto TiO₂ requires a temperature of at least 300–350 °C since its Tammann temperature is 261 °C.¹⁷ During methanol oxidation, crystalline MoO₃ spreads onto the TiO₂ surface as a surface molybdenum oxide species at a temperature even as low as 100 °C (see Figure 6). The possibility of any hot spots in the fixed-bed reactor can be ruled out because the methanol conversion is negligible at 100 °C and <5% at 150 °C, and thus, the exothermic heat of reaction is negligible. Thus, reaction-induced spreading of metal oxides during methanol oxidation generally occurs at much lower temperature than thermal spreading of metal oxides. The temperatures of 100–150 °C are significantly lower than the Tammann temperature of crystalline MoO₃, which indicates that thermal-induced spreading does not account for this phase transformation and that a strong interaction between the gas-phase components and crystalline MoO₃ must be occurring. Increasing the methanol oxidation reaction temperature from 100 °C to 230 °C leads to a significant increase in the extent of spreading (see Figure 6).

The bulk metal oxides (MoO₃, V₂O₅, and Cr₂O₃) do not thermally spread onto oxide supports at 230 °C because of their higher Tammann temperatures (listed in Table 1). Therefore, spreading of these metal oxides on the oxide supports (TiO₂ and SnO₂) during alcohol (methanol, ethanol, and 2-butanol) oxidation must correspond to the mechanism of reaction-induced spreading. For CrO₃ and Re₂O₇, thermal-induced spreading is probably also occurring during methanol oxidation at 230 °C due to their relatively low Tammann temperatures (-38 and 12 °C, respectively).

The reaction-induced spreading of bulk MoO₃ and V₂O₅ on TiO₂ and SnO₂ also readily occurs in the pellet catalysts during methanol oxidation at 230 °C (see Figures 7, 11, 13, and Table 2), despite mass transfer limitations in the pellets because of the rapid spreading of bulk MoO₃ and V₂O₅ during methanol oxidation.

Effect of the Gaseous Components. Several research groups found that the presence of water vapor influences the spreading rate of bulk MoO₃,^{16,40–42} WO₃,¹⁶ and V₂O₅,^{16,43} onto various oxide supports, but moisture is not essential for thermal spreading. These authors suggested that volatile metal oxyhydroxide intermediates such as MoO₂-

(OH)₂, WO₂(OH)₂, V₂O₃(OH)₄, and VO(OH)₃ formed in the presence of water vapor may play an important role in the chemical transformation of these metal oxides. The results presented in Figures 9 and 15 clearly show that the influence of water vapor on the spreading of bulk MoO₃ and V₂O₅ is negligible when the physical mixtures were heated in a water-vapor saturated O₂/He flow at mild temperatures such as 230 °C for a few hours.

The methanol oxidation reaction products are known to weakly interact with metal oxides such as molybdates and vanadates. Adsorbed formaldehyde is readily displaced by the presence of moisture and methanol.^{44,45} The interaction of carbon dioxide with molybdates and vanadates is extremely weak, and adsorption is usually not even observed at room temperature.^{46,47} Furthermore, reaction-induced spreading was observed during methanol oxidation even at 100 °C where no formaldehyde, carbon oxides, and water were produced. Thus, reaction-induced spreading is independent of the presence or absence of the methanol oxidation reaction products (HCHO, H₂O, CO, and CO₂).

The interaction of methanol with molybdates and vanadates, however, is very strong and is much stronger than moisture since adsorption of methanol readily displaces adsorbed moisture.^{44,45} Methanol oxidation over V₂O₅/SiO₂ and MoO₃/SiO₂ catalysts and crystalline MoO₃ and V₂O₅ results in the deposition of molybdena and vanadia at the cooler exit regions of the reactor due to the formation of volatile Mo(OCH₃)_n and V(OCH₃)_n complexes.¹⁰ In this work, crystalline MoO₃ and V₂O₅ were essentially removed from the V₂O₅/SiO₂ and MoO₃/SiO₂ physical mixture catalysts during methanol oxidation and deposited at the cooler exit regions of the reactor (see Figure 12B). Thus, the low-temperature dispersion of bulk metal oxides over oxide supports during methanol oxidation is considered to be related to the formation of the volatile metal–methoxy complexes. The methoxy complexes of vanadia and molybdena are well-known, and most of them are stable liquids possessing high vapor pressures at room temperature.⁴⁸ Thus, the presence of the TiO₂ and SnO₂ supports adsorb and stabilize the volatile metal–methoxy complexes through the formation of the surface metal–methoxy species.

The spreading of bulk MoO₃ and V₂O₅ onto TiO₂ induced by ethanol and 2-butanol is also due to the formation of volatile metal–alkoxy complexes. However, the kinetics of reaction-induced spreading of bulk MoO₃ on oxide supports during oxidation of higher alcohols are significantly slower relative to methanol oxidation (methanol > ethanol > 2-butanol). The lower spreading kinetics are related to the volatility and stability of the Mo–alkoxy complexes. As a rule of thumb, the volatility and stability of the corresponding alkoxide compounds decreases when the number of carbon atoms increases in the alcohol chains.⁴⁸ The rate-determining step during the catalytic oxidation of alcohols to their corresponding aldehydes or ketones involves breaking the α C–H bonds of the surface alkoxy intermediates, and the stability of this bond decreases with the number of carbon atoms coordinated to the α carbon increases.^{45,49} Thus, the methoxy complex

(43) Shan, S.; Honicke, D. *Chem.-Ing.-Techn.* **1989**, *61*, 321.(44) Cheng, W. H. *J. Catal.* **1996**, *158*, 477.(45) Holstein, W.; Machiels, C. J. *J. Catal.* **1996**, *162*, 118.(46) Segawa, K.; Hall, W. K. *J. Catal.* **1982**, *77*, 221.(47) Turek, A. M.; Wachs, I. E.; DeCanio, E. *J. Phys. Chem.* **1992**, *96*, 5000.(48) (a) Bradley, D. C.; Mehrotra, R. C.; Gaur, D. P. *Metal Alkoxides*; Academic Press: New York, 1978. (b) McCarron, E. M., III; Sleight, A. W. *Polyhedron* **1986**, *5*(1/2), 129. (c) Tatzel, G.; Greune, M.; Weidlein, J.; Jacob, E. *Z. Anorg. Allg. Chem.* **1986**, *533*, 83.(40) Margraf, R.; Leyrer, J.; Taglauer, E.; Knozinger, H. *Surf. Sci.* **1987**, *189*, 190, 842.(41) Leyrer, J.; Zaki, M. I.; Knozinger, H. *J. Phys. Chem.* **1986**, *90*, 4775.(42) Leyrer, J.; Mey, D.; Knozinger, H. *J. Catal.* **1990**, *124*, 349.

Table 2. Reaction-Induced Spreading of Some Metal Oxide/Support Systems during Methanol Oxidation

oxide	support	reaction temperature (°C)	Raman bands observed for surface species (cm ⁻¹)	spreading
MoO ₃	TiO ₂ (P-25)	100–230	950, 969	yes
	SnO ₂	230	970	yes
	SiO ₂	230		no
V ₂ O ₅	TiO ₂ (P-25)	230	938, 1018–1022	yes
	TiO ₂ (Anatase)	230	930	yes
	TiO ₂ (Rutile)	230	930	yes
	SnO ₂	230	1025	yes
	SiO ₂	230		no
CrO ₃	TiO ₂ (P-25)	230	1000	yes
Cr ₂ O ₃		230	1000	yes
Re ₂ O ₇		230	980, 990	yes
Nb ₂ O ₅		230, 400		no
WO ₃		230		no

is more stable than the ethoxy complex, and the ethoxy complex is more stable than the 2-butoxy complex. Consequently, the greater volatility and stability of M-methoxy complexes are responsible for the faster reaction-induced spreading kinetics observed during methanol oxidation.

Effect of Oxide Supports. The current studies reveal that reaction-induced spreading of bulk MoO₃ and V₂O₅ readily occurs on TiO₂ and SnO₂ supports, but is not observed for the SiO₂ support. The previous work on thermal spreading also claimed that surface metal oxide species could not be readily achieved on the SiO₂ support and, thus, conflicting results have been reported in the catalysis literature.^{7,8,16,22,50} Several research groups demonstrated that salts and metal oxides (especially bulk MoO₃) could spread onto SiO₂ when their physical mixtures were heated.^{8,9} However, other authors excluded the possibility of thermal spreading of bulk metal oxides on SiO₂.⁹ Consequently, alternate preparation methods such as impregnation and gas-phase grafting have been widely used to achieve higher dispersions of metal oxides onto the SiO₂ surface. Furthermore, the surface metal oxide species on SiO₂ is not thermally stable because physical mixtures of SiO₂-supported metal oxides with other oxide supports result in complete migration of the surface metal oxide species from SiO₂ to the other oxide supports (e.g., TiO₂) upon thermal treatment.⁵¹ The difficulty of wetting the SiO₂ surface by other metal oxides is related to the low interaction energy between the metal oxides and SiO₂ due to the hydrophobic character, low surface OH density, and reactivity of the SiO₂ surface.¹⁰

The stability of the surface metal oxide species on SiO₂ in the presence of water and alcohol vapors is extremely low and is reflected by the observation that water and methanol can transform the surface metal oxide species to crystalline bulk metal oxides through the formation of mobile and volatile metal oxide species.^{12,26,52} During methanol oxidation over silica-supported catalysts, the transformation of surface metal oxide species to their corresponding bulk metal oxides is dominant, and its reverse process of reaction-induced spreading is essentially absent. Therefore, there is a good correlation between reaction-induced spreading and the stability of surface metal oxide species on a specific support in the presence of alcohols. This relationship allows us to classify the oxide supports in two groups: group I consists of only SiO₂ on which the surface metal oxide species is not stable in the

presence of alcohols and reaction-induced spreading does not occur during alcohol oxidation reactions, and group II consists of TiO₂, SnO₂, Al₂O₃, ZrO₂, and CeO₂ that favor and stabilize the surface metal oxide species in the presence of alcohols and reaction-induced spreading readily occurs during alcohol oxidation reactions.

The specific TiO₂ phase (anatase and rutile) does not influence the reaction-induced spreading kinetics of bulk V₂O₅ because the same surface vanadium oxide species is present on both anatase and rutile TiO₂ supports after methanol oxidation (see Table 2). Previous structure–reactivity studies also reveal that the TiO₂ phases (anatase, rutile, brookite, and B) do not influence the molecular structure and reactivity of the surface vanadium oxide species.⁵³

Effect of Bulk Metal Oxides. Metal oxides with lower melting points and Tammann temperatures (e.g., CrO₃, MoO₃, V₂O₅, and Re₂O₇) can readily spread onto TiO₂ as the surface metal oxide species during methanol oxidation at 230 °C. In contrast, metal oxides with higher melting points and Tammann temperatures (e.g., WO₃ and Nb₂O₅) do not readily transform into the surface metal oxide species on TiO₂ during methanol oxidation reactions at the same temperature (see Table 2). The metal oxides with higher melting points imply a higher stability of the crystalline structures due to their high cohesive or lattice energies. Transformation from a crystalline state into an amorphous surface metal oxide species requires a much stronger interaction between the metal oxides and the gaseous components than the interaction among the crystalline lattices, which were not fulfilled in current methanol reaction conditions.

The oxidation state of the cations in the bulk metal oxides is not as important in reaction-induced spreading as in thermal spreading since thermal spreading is significantly retarded for reduced metal oxide phases that usually possess very high Tammann temperatures.^{9,39} However, essentially complete dispersion of bulk V₂O₅ on TiO₂ was observed during methanol oxidation even though the in situ Raman spectra revealed that the vanadia was reduced under the reaction conditions (see Figure 13). Essentially complete dispersion of bulk MoO₃ on TiO₂ was also observed after treatment of the catalyst in an oxygen-free methanol environment (see Figure 9). Furthermore, reaction-induced spreading of bulk Cr₂O₃, a reduced bulk metal oxide, on TiO₂ was observed to occur during methanol oxidation even at 230 °C (see Table 2). In view of the extremely high Tammann temperature of Cr₂O₃ (1081 °C), thermal spreading should be infeasible at such a mild temperature. The literature previously suggested

(49) Farneth, W. E.; Staley, R. H.; Sleight, A. W. *J. Am. Chem. Soc.* **1986**, *108*, 2327.

(50) Knozinger, H. *Mater. Sci. Forum* **1988**, *25/26*, 223.

(51) Jehng, J. M.; Wachs, I. E.; Weckhuysen, B. M.; Schoonheydt, R. A. *J. Chem. Soc., Faraday Trans.* **1994**, *91*, 953.

(52) Wang, C. B.; Deo, G.; Wachs, I. E. *J. Catal.* **1998**, *178*, 640.

(53) Deo, G.; Turek, A. M.; Wachs, I. E.; Machej, T.; Haber, J.; Das, N.; Eckert, H.; Hirt, A. M. *Appl. Catal., A* **1992**, *91*, 27.

that CrO_2 ($T_{\text{Tam}} = -36\text{ }^\circ\text{C}$) and CrO_3 ($T_{\text{Tam}} = -38\text{ }^\circ\text{C}$) might be the mobile phase assisting the spreading process of Cr_2O_3 under certain circumstances.⁵⁴ Thus, reaction-induced spreading of Cr_2O_3 during methanol oxidation might be assisted by trace amounts of surface CrO_3 and/or CrO_2 that have low Tammann temperatures through the formation of Cr-methoxy complexes. Therefore, the oxidation states of the metal oxides do not significantly influence the kinetics of reaction-induced spreading of crystalline metal oxides and reaction-induced spreading must proceed by mechanisms different from thermal spreading.

4.2.2. Driving Force and Mechanisms of Reaction-Induced Spreading. Similar to thermal spreading, reaction-induced spreading is a solid-state wetting (solid/solid adsorption) phenomenon, and thus, the driving force for reaction-induced spreading is also a decrease in the overall surface free energy or a concentration gradient of the dispersed metal oxide.^{7,8} However, the kinetics of reaction-induced spreading are modified by interaction (or reaction) of alcohol with spreading metal oxides.

As discussed above, alcohols (methanol, ethanol, and 2-butanol) possess the functional C-OH groups that are responsible for the efficient transformation of bulk crystalline metal oxides into the two-dimensional surface metal oxide species on oxide supports via the formation of M-alkoxy complexes. Reaction-induced spreading of a bulk metal oxide onto an oxide support surfaces assisted by alcohol involve the following steps: (a) attack of the crystalline metal oxide by alcohol molecules to form M-alkoxy complexes, (b) transfer of the M-alkoxy complexes from the crystalline metal oxide to the oxide-support surfaces, and (c) transformation of the M-alkoxy complexes into surface metal oxide species to stabilize on the oxide support surfaces.

Step b can be considered in the following two ways: (i) transport by surface diffusion or migration in a concentration gradient of the surface M-alkoxy complexes; (ii) gas-phase volatilization/readsorption of the volatile M-alkoxy complexes. It is well-known that metal-alkoxy species are the reaction intermediates of alcohol oxidation over supported metal oxide catalysts.⁵⁵ The mobility of the surface M-alkoxy complexes is directly related to the number of alkoxy groups attached to the metal cation. The greater the number of alkoxy groups, the more mobile the surface M-alkoxy complexes will be. Even volatile M-alkoxy compounds could form under alcohol oxidation conditions, as evident from the observation that bulk MoO_3 and V_2O_5 can be transported from the reactor to the cooler exit of the reactor during methanol oxidation. In the case of physical mixture, the oxide supports can trap the gas-phase M-alkoxy compounds to react with their surface hydroxyls,¹⁰ resulting in formation of surface M-alkoxy complexes. The dramatic temperature difference between reaction-induced spreading and thermal-induced spreading is directly related to the mobile M-alkoxy complexes formed during alcohol oxidation.

The mechanism of reaction-induced spreading corresponds to a mechanism previously proposed for thermal spreading.³⁸ The authors assumed thermal spreading to contain two steps: (a) a "molecule" leaves its metal oxide surface for the external surface of a support and (b) the "molecule" further diffuses on the support surface. It was found that for solid compounds with high melting points

step a is the rate-determining step and that for compounds with low melting points step b is the rate-determining step. The presence of alcohols can greatly facilitate the first step as well as the second step by formation of mobile metal-alkoxy complexes or volatile alkoxide as transporting intermediates, and thus, the activation energy and temperature required for spreading are dramatically decreased with assistance of alcohols.

4.2.3. Catalytic Properties. It has been well documented that the surface metal oxide species of the supported metal oxide catalysts are the active sites, which control the catalytic properties.⁶ The current studies clearly demonstrate that the methanol oxidation activity and the formaldehyde selectivity of the binary oxide physical mixture catalysts asymptotically approach the catalytic properties of their corresponding supported metal oxide catalysts prepared by impregnation (100% dispersion) (see Figures 8A and 14A). The changes in the catalytic properties as a function of reaction time correspond to the transformation of the active components from three-dimensional metal oxides into two-dimensional surface metal oxide species on the oxide supports (e.g., TiO_2 and SnO_2). The final methanol TOF and formaldehyde selectivity of the 4% $\text{V}_2\text{O}_5/\text{TiO}_2$ physical mixture catalyst are essentially the same as those of the 4% $\text{V}_2\text{O}_5/\text{TiO}_2$ supported catalyst prepared by impregnation, suggesting that essentially all of the crystalline metal oxides spread onto the TiO_2 surface as surface vanadium oxide species (see Figure 14A). The Raman spectrum of the final catalyst confirms the complete spreading of crystalline V_2O_5 (see Figure 14B). However, changes in catalytic properties with reaction time were not observed for the physical mixture catalysts comprised of bulk metal oxides and the SiO_2 support because the surface metal oxide species did not form on the SiO_2 surface during methanol oxidation (see Figure 12 and Table 2). The data in Figures 10 and 16 also reveal that the conversions of ethanol and 2-butanol oxidation reactions over the physical mixture catalysts increase with reaction time, implying the occurrence of an analogous transformation from three-dimensional metal oxides into the active surface metal oxide species during the alcohol oxidation reactions.

In the catalysis literature, synergetic effects involving oxygen spillover of active species in selective oxidations over mixed metal oxide catalysts have been proposed to play a determining role in catalysis.^{56,57} This phenomenon might be related to reaction-induced spreading, where one metal oxide migrates or "spills over" to the surface of another metal oxide. The possibility that reaction-induced spreading occurs during selective oxidation reactions over physical mixture catalysts needs to be carefully examined and eliminated before other mechanisms are proposed to explain the observed synergetic effects of physical mixture catalysts.

4.2.4. Implications for Catalyst Preparation. A very important consequence of reaction-induced spreading of bulk metal oxides during alcohol oxidation is that the catalyst preparation method of many supported metal oxide systems is not critical since the same surface metal oxide species will form during oxidation reactions (especially methanol oxidation). The current findings that reaction-induced spreading of bulk metal oxides on oxide supports can occur during oxidation reactions, especially methanol oxidation, at very low temperatures also have important implications for commercial applications. They provide an alternate and unique route for the preparation

(54) (a) Fouad, N. E.; Knozinger, H.; Ismail, H. M.; Zaki, M. I. Z. *Phys. Chem.* **1991**, *173*, 201. (b) Jozwiak, W. K.; Dalla Lana, I. G. *J. Chem. Soc., Faraday Trans.* **1997**, *93*, 2583.

(55) (a) Tatibouet, J. M. *Appl. Catal.*, **A** **1997**, *148*, 213. (b) Zhang, W., Oyama, S. T. *J. Phys. Chem.* **1996**, *100*, 10759.

(56) Ruiz, P.; Delmon, B. *Catal. Today* **1988**, *3*, 199.

(57) Delmon, B.; Froment, G. F. *Catal. Rev.-Sci. Eng.* **1996**, *38*, 69.

and manufacture of supported metal oxide catalysts, where handling a large volume of salt solution in aqueous impregnation and coprecipitation methods and using expensive precursors in an alkoxide impregnation can be avoided and, therefore, offers an environmental benign and economic process for catalyst preparation.

5. Conclusions

A new phenomenon of reaction-induced spreading of bulk metal oxides on oxide supports as a two-dimensional metal oxide overlayer was observed during alcohol oxidation at temperatures much lower than that required for thermal spreading. The reaction-induced spreading proceeds through formation, surface diffusion and volatilization/readsorption of metal-alkoxy complexes. Many factors (e.g., catalyst temperature, gaseous component, oxide support, and metal oxide) were found to influence the transformation kinetics of three-dimensional crystalline metal oxides into two-dimensional surface metal oxide species. Increasing the reaction temperature increases the spreading rate. The gaseous components assist the metal oxide spreading in the following order: methanol \gg ethanol $>$ 2-butanol, water \gg oxygen, helium. The high effectiveness of methanol-assisted spreading corresponds to the high volatility and stability of the metal-methoxy complexes. There are two categories of oxide supports: (1) SiO_2 , on which the reaction-induced spreading does not occur and the reverse process of transformation of

surface metal oxide species to crystallites dominates; (2) oxide supports (e.g., TiO_2 and SnO_2), where reaction-induced spreading of bulk metal oxides (e.g., CrO_3 , Cr_2O_3 , MoO_3 , V_2O_5 , and Re_2O_7) readily occurs during alcohol oxidation at mild temperatures. Bulk WO_3 and Nb_2O_5 do not readily transform into surface metal oxide species during alcohol oxidation due to their high cohesive and lattice energies. The oxidation states of the spreading metal oxides do not appear to influence the kinetics of reaction-induced spreading. The alcohol oxidation catalytic properties were found to correspond to the transformation of crystalline metal oxides into the surface metal oxide species, which are the active sites for alcohol oxidation. Both methanol oxidation activity and formaldehyde selectivity of the physical mixture catalysts can reach those of their corresponding supported metal oxide catalysts after sufficient exposure to the reaction environment. Supported metal oxide catalysts can be made using reaction-induced spreading as an alternate and unique route to avoid handling large amounts of salt solutions during coprecipitation and the use of expensive precursors in alkoxide impregnation.

Acknowledgment. Financial support of the Division of Basic Energy Sciences of the Department of Energy, grant DEFG02-93ER 14550, is gratefully acknowledged.
LA9807210